

# Extraordinary magnetoresistance of organic semiconductors : Hopping conductance via non-zero angular momentum orbitals

A. S. Alexandrov<sup>\*,1,2</sup>, V. A. Dediu<sup>3</sup>, V. V. Kabanov<sup>2</sup>, R. R. da Silva<sup>1</sup> and Y. Kopelevich<sup>1</sup>

<sup>1</sup> *Instituto de Física Gleb Wataghin, Universidade Estadual de Campinas,*

*UNICAMP 13083-970, Campinas, Sao Paulo, Brasil*

<sup>2</sup> *Josef Stefan Institute, 1001 Ljubljana, Slovenia*

<sup>3</sup> *ISMN-CNR, Via Gobetti 101, 40129 Bologna, Italy*

Highly-anisotropic in-plane magneto-resistance (MR) in graphite (HOPG) samples has been recently observed (Y. Kopelevich *et al.*, arXiv:1202.5642) which is negative and linear in low fields in some current direction while it is giant, super-linear and positive in the perpendicular direction. In the framework of the hopping conductance theory via non-zero angular momentum orbitals we link extraordinary MRs in graphite and in organic insulators (OMAR) observed in about the same magnetic fields. The theory predicts quadratic negative MR (NMR) when there is a time-reversal symmetry (TRS), and linear NMR if TRS is broken. We argue that the observed linear NMR could be a unique signature of the broken TRS both in graphite and organic compounds. While some local paramagnetic centers are responsible for the broken TRS in organic insulators, a large diamagnetism of our HOPG samples may involve a more intriguing scenario of TRS breaking.

PACS numbers: 72.20.Ee, 72.80.Le, 72.20.My, 73.61.Ph

## I. INTRODUCTION

Transverse resistance,  $R(B)$ , of isotropic conductors with Bloch electrons increases with an applied magnetic field so that  $MR \equiv R(B)/R(0) - 1$  is positive and quadratic in  $B$  [2]). A large positive MR is also used to be a hallmark of the hopping conductance in doped insulators [4]. While the carrier s-wave function on a donor (or acceptor) is spherically symmetric in the absence of the magnetic field, it becomes cigar-shaped squeezed in the transverse direction to the field [5–9]. This leads to a significant decrease in the overlap of the wave-function tails of two neighboring donors, and hence to a significant increase of resistivity (positive MR), which is also quadratic in low magnetic fields.

However there are exceptions which do not show these canonical MRs. For instance some semiconductors and semimetals (e. g. bismuth), where open Fermi surfaces are unfeasible, show positive but linear MR. One of the theoretical possibilities for such a phenomenon is a so-called quantum magnetoresistance in semimetals having pockets of the Fermi surface with a small or even zero effective mass (as the Dirac fermions in bismuth, graphite and graphene), which might be in the ultra-quantum limit at rather low magnetic fields [10].

Also there is anomalous *negative* MR (NMR) observed in some hopping systems, for instance in amorphous germanium and silicon. Originally it has been attributed to magnetic-field dependence of spin-flip transitions between sites when some fraction of them has a frozen spin [11], and/or to an increase of the density of localised states due to the Zeeman energy shift,  $\mu_B B$  [12]. This NMR is used to be small (much less than 1%) even in relatively high magnetic fields of about 1 Tesla. There are other theoretical mechanisms of NMR, in particular the weak localization gives NMR which is often almost linear in a certain field range. Such NMR smoothly

evolves from a sub-linear magnetic field dependence at lower temperatures to super-linear field dependence at higher temperatures. A strong NMR exists in the classical two-dimensional electron gas due to freely circling electrons, which are not taken into account by the Boltzmann approach. It is parabolic rather than linear at low fields [13]. The parabolic orbital NMR has been also predicted by the gauge theory in two-dimensional strongly-correlated doped Mott insulators [14].

More recently a linear NMR has been observed in the longitudinal c-axis inter-layer current in the normal state of cuprate superconductors and in graphite in high magnetic fields assigned to bipolarons in the former case [15] and to a growing population of the zero-energy Landau level of quasi-two-dimensional Dirac fermions with the increasing magnetic field in the latter case [16]. Also a giant transverse NMR of nearly 100% was observed at low temperatures, with over 50% remaining at room temperature in graphene nanoribbons and attributed to some delocalization effect under the perpendicular magnetic field [17].

Puzzling magnetoresistance effects in several different  $\pi$ -conjugated polymer and small molecular thin film devices have been observed named organic magnetoresistance (OMAR) [18]. OMAR reaches 10% at fields on the order of only 10 mT, and can be either positive or negative, depending on operating conditions. The effect is independent of the sign and direction of the magnetic field. The Zeeman energy does not account for the observed OMAR at ambient temperatures since it is too small,  $\mu_B B \approx 10$  mK, in the field of 10 mT. The observation of OMAR in hole-only devices [18, 19] indicates, on the other hand, that the effect is hardly compatible with an exciton-based mechanism.

An alternative model involving spin-dependent bipolaron formation in deep potential wells has been proposed as a possibility [19]. In this model bipolarons (i.e doubly

occupied sites) block single polaron transport through bipolaron states causing positive MR, while an increase in polaron population at the expense of bipolarons with increasing magnetic field might cause negative MR, if the long-range Coulomb repulsion around each carrier is sufficiently strong. However, one might expect that this mechanism should depend strongly on the carrier density, whereas OMAR is only weakly dependent on current density [18]. Finding a convincing explanation of OMAR is crucial for a better understanding of charge transport in organic semiconductors, actively used in light-emitting diodes, photovoltaic cells, field-effect transistors, and in spintronics [21, 22].

Recently an unusual orbital MR in HOPG has been observed [23]. In some current direction it is negative and linear in low fields with the crossover to the positive MR at higher fields, while in the perpendicular current direction MR is giant, super-linear and positive. In this paper we compare OMAR and graphite MR and propose an explanation of both MRs in the framework of the hopping magneto-conductance via non-zero angular momentum orbitals [24].

## II. HOPPING MAGNETOCONDUCTANCE VIA NON-ZERO ANGULAR MOMENTUM ORBITALS

In organic and inorganic doped insulators lattice defects such as vacancies, interstitials, and excess neutral atoms or ions often localise carriers in finite momentum states rather than in the zero-momentum s-state [25]. Also the conventional nonmagnetic donors and acceptors have nonzero orbital momentum states along with s-states, which are accessible for the hopping conduction at elevated temperature. Here we briefly outline the theory of hopping MR via non-zero angular momentum orbitals [24].

In the hopping regime with localized carriers MR is caused by a strong magnetic field dependence of the exponential asymptotics of bound state wave functions at a remote distance from a donor (or an acceptor). The asymptotics is found using the Green function,  $G(\mathbf{r}, \mathbf{r}'; E)$ , (GF) of free (or Bloch) electrons in the magnetic field with a negative binding energy  $E$  [4]. The three-dimensional GF,  $G_{3D}(\mathbf{r}, \mathbf{r}'; E)$  is readily calculated using the Fourier transformation of the two-dimensional  $G_{2D}(\vec{\rho}, \vec{\rho}'; E)$  [26],

$$G_{3D}(\mathbf{r}, \mathbf{r}'; E) = \frac{1}{2\pi\hbar} \int_{-\infty}^{\infty} dp e^{ip(z'-z)} G_{2D}\left(\vec{\rho}, \vec{\rho}'; E - \frac{p^2}{2m_b}\right) \quad (1)$$

$$G_{2D}(\vec{\rho}, \vec{\rho}'; E) = \frac{m_b}{2\pi\hbar^2} \exp\left[i\frac{\rho\rho'\sin(\phi' - \phi)}{2l^2}\right] \times e^{-(\vec{\rho} - \vec{\rho}')^2/4l^2} \Gamma(a) U[a, 1, (\vec{\rho} - \vec{\rho}')^2/2l^2], \quad (2)$$

where  $\phi$  and  $\phi'$  are azimuth angles of  $\vec{\rho}$  and  $\vec{\rho}'$  respectively,  $l = (\hbar/eB)^{1/2}$  is the magnetic length,  $\Gamma(a)$  is the

gamma-function,  $U(a, b, z)$  is the Tricomi's confluent hypergeometric function well-behaved at infinity,  $z \rightarrow \infty$ , for negative  $E$ , and  $a = 1/2 - (E \mp \mu_B B)/\hbar\omega_c$  ( $\mp$  corresponds to spin up/down, respectively). Neglecting a small diamagnetic correction (quadratic in  $B$ ) yields

$$E = -\epsilon_0 + \hbar\omega_c m/2 \pm \mu_B B, \quad (3)$$

where  $\omega_c = eB/m_b$  ( $m_b$  is the band mass),  $m = 0, \pm 1, \pm 2, \dots$  is the magnetic quantum number of the localised state so that

$$a = \frac{1}{b} + \frac{1-m}{2}. \quad (4)$$

Hereafter we measure the magnetic field,  $b = B/B_0$ , in units of  $B_0 = \hbar\kappa^2/2e$ , where  $\kappa = (2m_b\epsilon_0)^{1/2}/\hbar$  is the inverse localisation length of the zero-field state with the ionisation energy  $\epsilon_0$ .

Now using an integral representation of the confluent hypergeometric function [27] one obtains after integrating over  $p$  in Eq.(1)

$$G_{3D}(\mathbf{r}, 0; E) = \frac{m_b}{(2\pi)^{3/2}\hbar^2 l} \int_0^\infty dx \frac{e^{mx}}{\sqrt{x} \sinh(x/2)} \times \exp\left\{-\left[\frac{(\kappa\rho)^2 b}{8} + \frac{x}{b} + \frac{(\kappa z)^2 b}{4x} + \frac{(\kappa\rho)^2 b}{4(e^x - 1)}\right]\right\}. \quad (5)$$

Expanding the exponent in the square brackets in Eq.(5) up to the third power in  $x$  and performing the integration by the saddle-point method we obtain the asymptotics of the 3D impurity wave function,  $\psi(\mathbf{r}, B) \propto G_{3D}(\mathbf{r}, 0; E)$  at  $1 \ll \kappa r \lesssim 1/b$  as [24]

$$\psi_m(\mathbf{r}, B) \propto \psi_m(\mathbf{r}, 0) \frac{\kappa r b/2}{\sinh(\kappa r b/2)} \exp\left[\frac{m\kappa r b}{2} - \frac{\kappa^3 \rho^2 r b^2}{96}\right] \quad (6)$$

with  $r^2 = \rho^2 + z^2$ .

For the s-wave bound state with  $m = 0$  this is the textbook asymptotics [4, 9] accounting for the conventional positive MR quadratic in small  $B$ . On the contrary, for orbitals with nonzero orbital momentum the wave function, Eq.(6), is *linear* in small  $B$ . Remarkably a localized state with a positive  $m$  expands in the magnetic field due to the magnetic lowering of its ionization energy by  $\hbar\omega_c m/2$ , while states with negative  $m$ s shrink. The linear term dominates in a wide range of realistic impurity densities for any nonzero  $m$  because of the small numerical factor (1/96) in the quadratic term in the exponent of Eq.(6).

The hopping integral is proportional to  $\psi_m(\mathbf{r}, B)$ , where  $r$  is the distance between two hopping sites, which is assumed to be large compared with the localisation length. The hopping conductance is proportional to the hopping integral squared. If there is no time-reversal symmetry breaking, the states with the opposite direction of the orbital angular momentum,  $m$  and  $-m$ , are degenerate, so that the linear term in the conductivity,

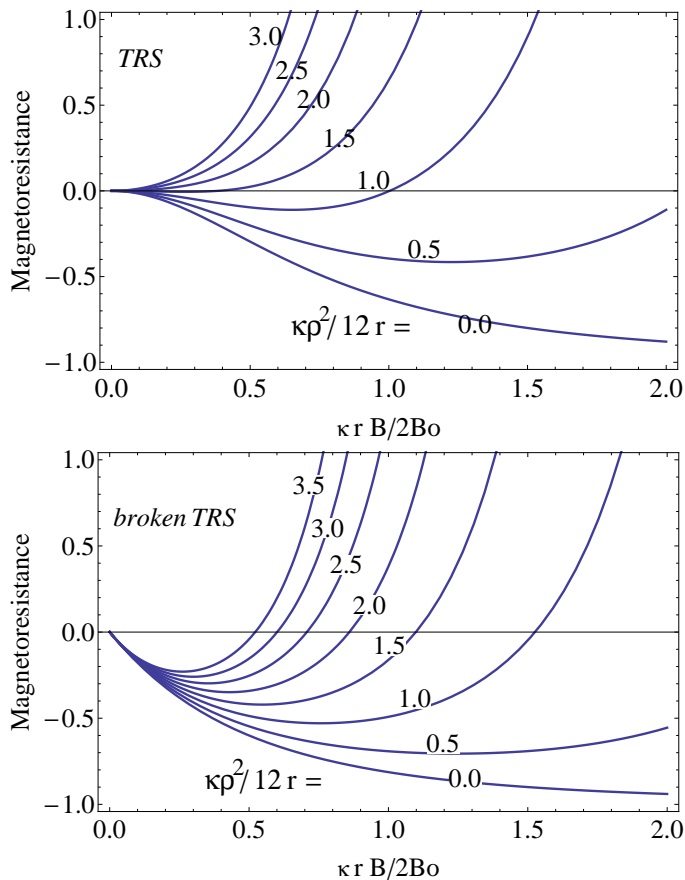


FIG. 1: Upper panel: Magnetoresistance to hopping via  $p$ -orbitals in TRS systems versus the magnetic field. Lower panel: The same MR in systems with the broken TRS.

$\sigma = \sigma_m + \sigma_{-m}$  cancels, and

$$\sigma(B) = \sigma(0) \left[ \frac{\kappa r b / 2}{\sinh(\kappa r b / 2)} \right]^2 \cosh(m \kappa r b) e^{-\kappa^3 \rho^2 r b^2 / 48}. \quad (7)$$

In this case the hopping conductivity,  $\sigma(B)$  first *increases* quadratically with the magnetic field (parabolic NMR) and only then decreases with  $B$  (positive MR), if  $\kappa \rho^2 / r < 24m^2 - 4$  as illustrated in Fig.1 (upper panel) representing  $MR = \sigma(0) / \sigma(B) - 1$  for  $p$ -states ( $m = \pm 1$ ).

Ions that carry a magnetic moment break the time-reversal symmetry and split  $m$  and  $-m$  states. Such zero-field splitting (ZFS) gives preference to hopping via orbitals with a lower ionisation energy (positive  $m$ ). Hence in a ferromagnet with the *frozen* magnetisation MR for hopping via nonzero momentum orbitals is highly anisotropic changing from linear and negative in the field applied parallel to the magnetisation to linear but positive in the opposite field. On the other hand if the global or local internal magnetisation rotates with the external magnetic field (superparamagnetism) magnetoresistance is negative and linear in small  $\mathbf{B}$  no matter what the direction of the external field is. When the splitting due to

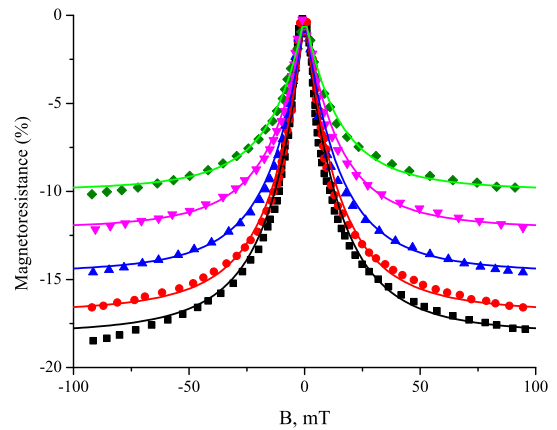


FIG. 2: (Color online) Magnetoresistance measured at room temperature in  $ITO/PEDOT/Alq3/Ca$  device at bias voltages 12, 13, 14, 15, 17 V (symbols from bottom to top, respectively, Ref.[18]) described by Eq.(10) (solid lines) with  $B_h = 30$  mT,  $m = 1$  and the resistance ratio  $R$  shown in Fig.3.

an internal (exchange) field is comparable or larger than the temperature, the hopping MR is found as

$$MRh = -1 + \left[ \frac{\sinh(\kappa r b / 2)}{\kappa r b / 2} \right]^2 \exp \left[ \kappa^3 \rho^2 r \frac{b^2}{48} - |m| \kappa r b \right]. \quad (8)$$

MRh in systems with the broken TRS, Eq.(8), shown in Fig.1 (lower panel), is quite distinguishable from MRh in TRS systems, Fig.1(upper panel).

### III. OMAR

Eq.(8) allows us to address puzzling experimental observations of negative NMR in a number of organic materials [18–20]. There is experimental evidence for paramagnetic centers and ZFS in polymers, in particular in Alq3 [28]. More recently dilute magnetic impurities and magnetic domains have been observed in some  $\pi$ -conjugated polymers [29]. Hence as suggested in Ref.[24], if TRS is broken by such magnetic centers, the low-field magnetoresistance is dominated by the linear NMR via non-zero angular momentum orbitals, Eq.(8). Here we extend our original description [24] of OMAR to the whole range of magnetic and electric fields used in the experiments.

The device fabrication [18–20] started with glass substrates coated with a metallic layer, indium-tin-oxide ITO or the conducting polymer PEDOT. The semiconducting polymer (e. g. Alq3) layer was thermally evaporated onto the bottom electrode, yielding an organic-semiconductor layer thickness of about 100 nm. The cathode, either Ca with an Al capping layer, Al, or Au

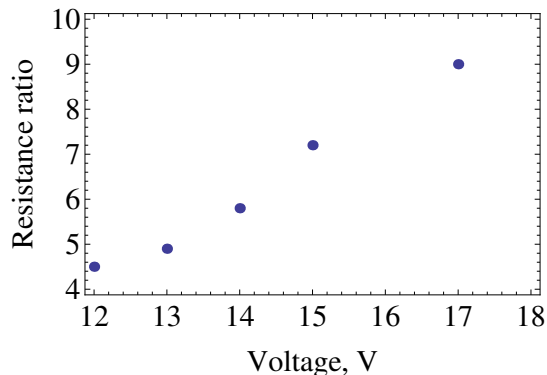


FIG. 3: Ratio of the zero-field resistance of other layers and contacts to the zero-field organic-semiconductor resistance.

was then deposited on top.

The resistance of the device is the sum of the hopping resistance,  $R_h$ , of the organic semiconductor layer probably including the interface, and of other layers and contacts,  $R_m$ . Hence, the magnetoresistance is expressed via metallic/contact  $MRm = R_m(B)/R_m(0) - 1$  and the hopping magnetoresistance,  $MRh$  of Alq3 as

$$MR = \frac{MRm}{1 + 1/R} + \frac{MRh}{1 + R}, \quad (9)$$

where  $R = R_m(0)/R_h(0)$  is the ratio of the zero-field resistance of other layers and contacts to the zero-field organic-semiconductor resistance. Reducing the number of fitting parameters we further assume that  $MRm$  is small,  $MRm \ll MRh$ , and the first term in Eq.(9) can be neglected. Also as outlined above the quadratic term in the exponent of Eq.(8) can be dropped in the relevant magnetic fields which yields

$$MR \approx \frac{(2B_h \sinh(B/2B_h)/B)^2 \exp(-|m|B/B_h) - 1}{1 + R}, \quad (10)$$

where  $B_h = B_0/\kappa r$  is the characteristic scaling field.

As shown in Fig.2 Eq.(10) with  $R$  as a single fitting parameter describes remarkably well the experimental NMR for all magnetic and electric fields used in the experiment. The resistance ratio  $R$  increases with the voltage,  $V$ , on the device, Fig.3, presumably due to a drop of the zero-magnetic field  $R_h(0)$  with  $V$ .

#### IV. GRAPHITE MR

Ref.[23] observed unusual MR in commercially available HOPG samples with different mosaicity and the room temperature out-of-plane/basal plane zero-field resistivity ratio  $\rho_c/\rho_{ab}$  as high as  $10^5$ . The magnetic field was applied parallel to the hexagonal c-axis ( $B \parallel c$ ), and the in-plane  $\rho_{ab}(B, T)$  was measured placing silver pasted electrodes on the sample surface. All resistance measurements were performed in the Ohmic regime (more sample

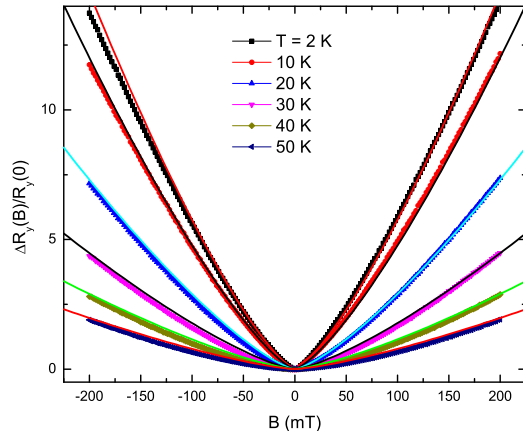


FIG. 4: (Color online) Giant in-plane magnetoresistance of HOPG in the metallic (Y) direction at different temperatures (symbols [23]) fitted with  $(B/B_{in})^{4/3}$  (lines).

details and complementary magnetization measurements are found in Ref.[23]).

The graphite samples described in Ref.[23] show qualitatively different temperature dependence of the in-plane zero-field resistance for the current in two perpendicular in-plane directions. In one direction (called here Y) the resistance is metallic-like while in the other direction (X) it is insulating-like in a wide temperature interval from 2K to the room temperature. Since a sufficiently strong magnetic field of about 1 Tesla or more makes graphene planes electrically isotropic the anisotropy is of electronic origin. The in-plane electrical anisotropy is most probably associated with an inhomogeneous carrier-density distribution, such that well doped metallic clusters are partially overlapped in Y-direction while they are separated by poorly doped insulating regions in X-direction. The in-plane anisotropy has been observed only in most anisotropic ( $\rho_c/\rho_b \approx 10^5$ ) graphite samples pointing to its quasi-2D origin. Our measured Kish and natural graphite crystals possess much lower resistivity ratio ( $\rho_c/\rho_b \approx 10^2 - 10^3$ ) with no such effect observed. No in-plane anisotropy has been observed in HOPG samples with  $\rho_c/\rho_b < 10^4$  either. It brings us to a conclusion that the electrical anisotropy is closely related to the reduced electron dimensionality in quasi-2D graphite providing a quasi-1D percolation in the planes.

When a relatively weak magnetic field is applied perpendicular to the planes, the MR along the metallic Y direction appears huge and positive, Fig.4. A giant positive MR is naturally expected in doped graphite with virtually massless Dirac fermions [30] since the parameter  $\beta = \omega_c \tau$  becomes large already in the mT-region of the field (here  $\tau$  is the scattering time). However, it is neither quadratic as in the Boltzmann theory, nor

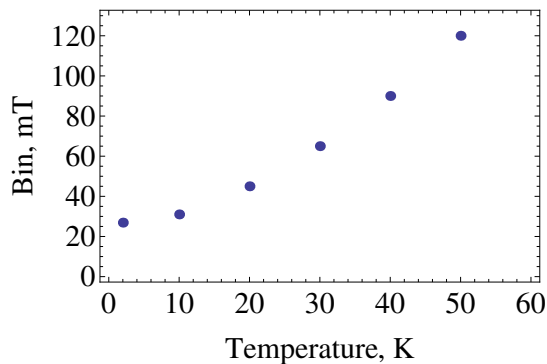


FIG. 5: Characteristic field  $B_{in}$  of metallic clusters in HOPG as a function of temperature.

linear in  $B$  as in the quantum magnetoresistance [10]. It has been suggested [23] that inhomogeneities are responsible for the strong departure from these regimes. They lead to a radical rearrangement of the current flow pattern changing the magnetic field dependence of the transverse conductivity. Importantly, when  $\beta > 1$ , then even relatively small inhomogeneities in the carrier density lead to the MR proportional to  $B^{4/3}$  [31]. In fact,  $MRy = (B/B_{in})^{4/3}$  perfectly fits the observed magnetic field dependence of MR in the metallic current direction, Fig.(4) with a single scaling parameter  $B_{in}$  depending on fluctuations in the carrier density [31] and temperature, Fig.5. The temperature dependence of  $B_{in}(T)$  is reminiscent of the temperature dependence of metallic resistivity, as it should be since  $B_{in} \propto 1/\tau$  [31].

The MR in the insulating direction is also anomalous, Fig.6. It is linear and negative in very low fields and positive and superlinear in higher fields above the crossover point. The insulating-like temperature dependence of the zero-field resistance [23] in this direction supports the view that the metallic clusters are virtually nonoverlapped along X, and the resistance is the sum of the hopping resistance,  $R_h$  of the insulating regions with low doping, and the metallic-like resistance  $R_m$ . Hence, the magnetoresistance in X direction is expressed via metallic MRy and the hopping magnetoresistance, MRh of insulating layers as in Eq.(9),

$$MRx = \frac{MRy}{1 + 1/R} + \frac{MRh}{1 + R}, \quad (11)$$

where  $R = R_m(0)/R_h(0)$  is the ratio of the zero-field metallic resistance to the zero-field insulating resistance. This ratio ranges from about 0.1 at 2K to 1 at room temperature [23].

However, different from OMAR Eq.(9) the first term in Eq.(11) is significant and responsible for the upturn of  $MRx$  from negative to positive at some magnetic field about 70 mT, Fig.(6) as described in Ref.[23]. Here we analyse in more detail the low-field asymptotics of  $MRx$ . If TRS is broken in HOPG then according to Eq.(10) this asymptotics is linear in  $B$  because the first term in

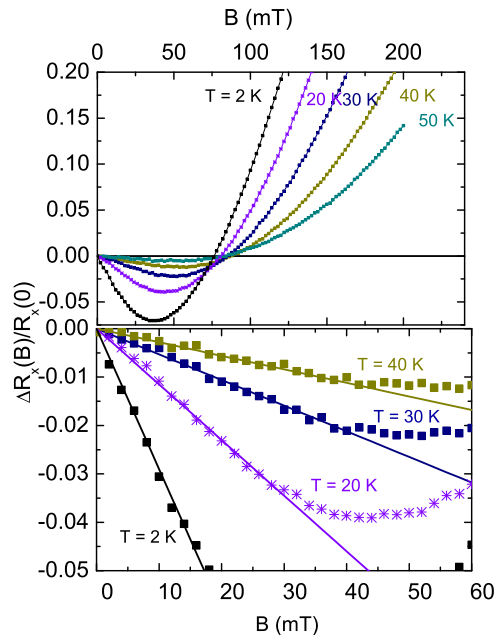


FIG. 6: (Color online) Upper panel: Magnetoresistance in the insulating (X) direction (symbols). Lower panel: Low-field negative linear MR fitted as  $MRx = -B/B_s$  with  $B_s = (1 + R)B_h/|m|$ , shown in Fig.7 at different temperatures, indicating the time-reversal symmetry breaking.

Eq.(11) is superlinear,

$$MRx \approx -\frac{|m|B}{(1 + R)B_h} \quad (12)$$

for  $B \rightarrow 0$ .

With increasing temperature the resistance ratio  $R$  increases and deeper localized states with a higher ionization energy become accessible for the hopping conduction, so that the slope  $1/B_s$  of the linear negative MR drops, as observed, Figs.(6,7).

## V. CONCLUSIONS

In conclusion, we described the unusual magnetoresistance of organic insulators (OMAR) [18–20] and the highly-anisotropic in-plane magnetoresistance of quasi-two dimensional HOPG graphite [23] using the same theory of hopping magneto-conductance via non-zero angular momentum orbitals [24]. While the theory with one or two scaling parameters provides accurate agreement with OMAR and the HOPG data, there are other theoretical mechanisms of NMR outlined in the introduction and beyond. Most of them explain NMR as some spin-correlation effects. Importantly, there is no NMR and virtually no MR in the same range of the magnetic

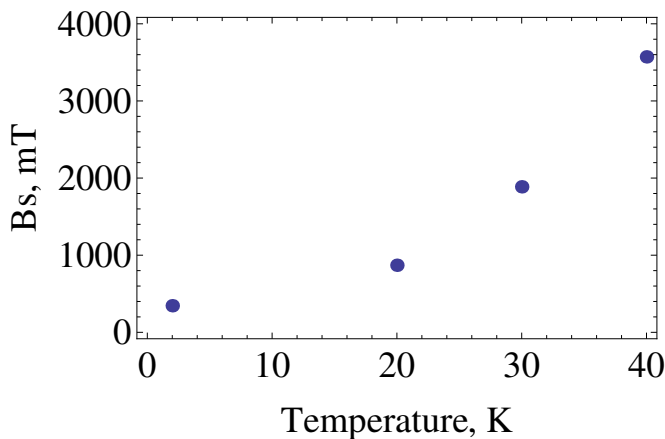


FIG. 7: Inverse slope  $B_s$  of the linear NMR in HOPG versus temperature.

field *parallel* to the planes, which rules out a spin origin of the observed NMR in our quasi-2D HOPG samples. Also there are no quantum magnetic oscillations at high temperatures, where unusual MRs are still observed, Figs.(4,6), so they are not related to the Landau quantization. In contrast to a number of spin correlation and weak localisation scenarios we observed the perfectly linear NMR at very low  $B$  in a wide temperature range, Fig.(6), which according to our theory is a clear signature of the time-reversal symmetry breaking.

The origin of the broken TRS in organic compounds and in graphite could be basically different. Instead of the (super)paramagnetism in polymers [28, 29] the graphite samples of Ref. [23] show a large diamagnetism. Naturally, some local paramagnetic centers responsible

for the broken TRS in organic semiconductors could be also found in graphite, with their magnetic response overwhelmed by the large diamagnetism of metallic clusters. However the observed large diamagnetism could suggest a more intriguing mechanism of TRS breaking, such as superconducting clusters [32] with an unconventional (chiral) order parameter [33, 34]. There is a kink in the field dependence of the diamagnetic magnetization of the HOPG samples at  $B_k \approx 0.2$  T, [23], resembling the behavior of type-II superconductors in magnetic fields exceeding the lower critical field. Supporting this possibility the electrically inhomogeneous samples are becoming homogeneous insulators in sufficiently high magnetic fields, which could suppress the superconductivity. Also in some 2D lattices there is the broken time-reversal symmetry (i.e. some internal magnetic ordering) in the normal state with a spontaneous quantum Hall effect but without any net magnetic flux at high temperatures [35]. At lower temperatures a pair of spontaneously generated current loops in adjacent graphene layers, having odd-parity with respect to the two layers, could also break TRS [36]

More generally our findings point to an inhomogeneous doping and a semiconducting gap in graphite.

#### Acknowledgements

This work has been supported by FAPESP, CNPq, CAPES, ROBOCON, INCT NAMITEC, the European Union Framework Programme 7 (NMP3-SL-2011-263104-HINTS), and by the UNICAMP visiting professorship programme.

- 
- [1] \* On leave from the Department of Physics, Loughborough University, Loughborough LE11 3TU, United Kingdom.
- [2] For some specific directions of  $\mathbf{B}$  the positive MR is linear in  $B$  [3] when the Fermi surface is open.
- [3] I. M. Lifshits and V. G. Peschanskii, Sov. Phys. JETP **8**, 875 (1959).
- [4] B. I. Shklovskii and A. L. Efros, *Electronic Properties of Doped Semiconductors*, Springer Series in Solid-State Science **45**(Springer-Verlag, Berlin, 1984), pp.155-179.
- [5] Y. Yafet, R. W. Keyes and E. N. Adams, J. Phys. Chem. Solids. **1**, 137 (1956).
- [6] R. J. Sladek, J. Phys. Chem. Solids. **5**, 157 (1958).
- [7] R. J. Elliot and R. Loudon, J. Phys. Chem. Solids. **15**, 196 (1960).
- [8] H. Hasegawa and R. E. Howard, J. Phys. Chem. Solids. **21**, 179 (1961).
- [9] N. Mikoshiba and S. Gonda, Phys. Rev. **127**, 1954 (1962).
- [10] A. A. Abrikosov, Europhys. Lett. **49** 789 (2000).
- [11] B. Movaghar and L. Schweitzer, J. Phys. C: Solid State Phys. **11**, 125 (1978).
- [12] A. Kurobe and H. Kamimura, J. Non-Crystalline Solids **59-60**, 41 (1983).
- [13] A. Dmitriev, M. Dyakonov, and R. Jullien, Phys. Rev. B **64**, 233321 (2001).
- [14] L. B. Ioffe and P. Wiegmann, Phys. Rev. B **45**, 519 (1992).
- [15] V. N. Zavaritsky, J. Vanacken, V. V. Moshchalkov, and A. S. Alexandrov, Physica C **404**, 444 (2004).
- [16] Y. Kopelevich, R. R. da Silva, J. C. M. Pantoja, and A. M. Bratkovsky, Phys. Lett. A **374**, 4629 (2010).
- [17] J. Bai, R. Cheng, F. Xiu, L. Liao, M. Wang, A. Shailos, K. L. Wang, Yu Huang, and X. Duan, Nature Nanotech. **5**, 655 (2010).
- [18] Ö. Mermer, G. Veeraraghavan, T. L. Francis, Y. Sheng, D. T. Nguyen, M. Wohlgenannt, A. Kehler, M. K. Al-Suti, and M. S. Khan, Phys. Rev. B **72**, 205202 (2005), and references therein.
- [19] P. A. Bobbert, T. D. Nguyen, F.W. A. van Oost, B. Koopmans, and M. Wohlgenannt, Phys. Rev. Lett. **99**, 216801 (2007).

- [20] T. D. Nguyen, Y. Sheng, J. Rybicki, and M. Wohlgenannt, Phys. Rev. B **77**, 235209 (2008).
- [21] V. Dediu, M. Murgia, F. C. Matocotta, C. Taliani, and S. Barbanera, Solid State Commun. **122**, 181 (2002).
- [22] M. Wohlgenannt, K. Tandon, S. Mazumdar, S. Ramasesha, and Z. V. Vardeny, Nature (London) **409**, 494 (2001).
- [23] Y. Kopelevich, R. R. da Silva and A. S. Alexandrov, arXiv:1202.5642.
- [24] A. S. Alexandrov, V. A. Dediu, and V. V. Kabanov, Phys. Rev. Lett. **108**, 186601 (2012).
- [25] A. Zunger, S. Lany, and H. Raebiger, Physics **3**, 53 (2010).
- [26] V. V. Dodonov, I. A. Malkin, and V. I. Manko, Phys. Lett. A **51**, 133 (1975); T. Ueta, J. Phys. Soc. Japan **61**, 4314 (1992)].
- [27] M. Abramowitz and I. A. Stegun, *Handbook of Mathematical Functions* (Dover Pub., New York 1970), pp.504-505.
- [28] M. N. Grecu, A. Mirea, C. Ghica, M. Cölle, and M. Schwoerer, J. Phys.: Condens. Matter **17** 6271, (2005).
- [29] S. Majumdar, H. Majumdar, J. O. Lill, J. Rajander, R. Laiho, and R. Österbacka, arxiv.org/abs/0905.2021.
- [30] I. A. Lukyanchuk and Y. Kopelevich. Phys. Rev. Lett. **93**, 166402 (2004).
- [31] Yu. A. Dreizin and A. M. Dykhne, Sov. Phys. JETP **36**, 127 (1973) [Zh. Eksp. Teor. Fiz. **63**, 242 (1972)].
- [32] Y. Kopelevich and P. Esquinazi, J. Low Temp. Phys. **146**, 629 (2007).
- [33] A. M. Black-Schaffer and S. Doniach, Phys. Rev. B **75**, 134512 (2007).
- [34] R. Nandkishore, L. S. Levitov, and A. V. Chubukov, Nature Physics **8**, 158 (2012).
- [35] F. D. M. Haldane, Phys. Rev. Lett. **61**, 2015 (1988).
- [36] L. Zhu, V. Aji, and C. M. Varma, arXiv:1202.0821.